Am J Transl Res 2022;14(6):3840-3853
www.ajtr.org /ISSN:1943-8141/AJTR0141694

Original Article

Stachydrine hydrochloride ameliorates cardiac hypertrophy through CaMKII/HDAC4/MEF2C signal pathway

Xue-Qin Li[1*], Shuang Lu[1*], Lei Xia[2], Xiao-Li Shan[3], Wen-Xia Zhao[1], Hui-Hua Chen[1], Chen Zhang[4], Wei Guo[4], Ming Xu[5], Rong Lu[1], Pei Zhao[3]

[1]School of Basic Medical Science, Shanghai University of Traditional Chinese Medicine, Shanghai, China; [2]Yueyang Hospital of Integrative Chinese and Western Medicine, Shanghai University of Traditional Chinese Medicine, China; [3]Public Laboratory Platform, School of Basic Medical Science, Shanghai University of Traditional Chinese Medicine, Shanghai, China; [4]Department of Pathology, Shanghai University of Traditional Chinese Medicine, China; [5]Department of Physiology, Shanghai University of Traditional Chinese Medicine, China. [*]Equal contributors.

Received January 11, 2022; Accepted March 31, 2022; Epub June 15, 2022; Published June 30, 2022

Abstract: Stachydrine hydrochloride (Sta), an activated alkaloid, is isolated from traditional Chinese medicine Yimucao. In previous studies, the cardioprotective effects of Sta were found in our laboratory. However, the underling mechanisms of Sta is not fully elucidated. The aim of this study was to provide a detailed account of the anti-hypertrophic effects of Sta on transcriptional regulation. In vivo, C57BL/6J mice were subjected to transverse aortic constriction (TAC) and were orally treated with Sta. Morphological assessments, echocardiographic parameters, histological analyses and immunofluorescence were used to evaluate cardiac hypertrophy. In vitro, cardiomyocytes were stimulated by phenylephrine (PE), and cell surface and hypertrophy markers were tested by immunofluorescence and real-time polymerase chain reaction (RT-PCR). Moreover, western blotting, RT-PCR and luciferase reporter genes were used to assess the expression of proteins, mRNA and the activity of the CaMKII/HDAC4/MEF2C signal pathway in vivo and in vitro. We found that Sta blocked cardiac hypertrophy induced by pressure overload. We also demonstrated that Sta inhibited nuclear export or promoted nuclear import of HDAC4 through regulation of p-CaMKII, and it further improved the repression of MEF2C. Taken together, our findings demonstrated that Sta ameliorates cardiac hypertrophy through CaMKII/HDAC4/MEF2C signal pathway.

Keywords: Cardiac hypertrophy, CaMKII/HDAC4/MEF2C signaling pathway, nuclear translocation, transcription regulation

Introduction

Heart failure (HF) is one of the leading causes of morbidity and mortality worldwide, and the prevalence of HF continues to rise over time. As a frequent precursor of HF, cardiac hypertrophy is characterized by an enlargement of the heart and thickening of the cardiac muscle, which are adaptive responses to various stimuli. Accumulating evidence suggests that the state of hypertrophy is compensatory by temporarily preserving cardiac output, but sustained pathological myocardial hypertrophy greatly increases the risk of HF, including sudden death [1, 2]. Although the current efficacy of treatment for cardiac hypertrophy is improving, the mortality rate 5 years after diagnosis remains at approximately 50% [3]. As an early stage of HF, hypertrophy has attracted increased attention, which leads to a call for earlier intervention in this process.

Hypertrophic agonists have been widely reported to elevate intracellular Ca^{2+} levels and stimulate Ca^{2+}-dependent pathways in cardiac myocytes [4]. Ca^{2+}/calmodulin-dependent protein kinase (CaMK), the cellular decoder of Ca^{2+} signals, plays an important role in cardiac diseases such as hypertrophic growth [4, 5]. CaMKII is the major isoform expressed in the heart and has been implicated in the transcriptional regulation associated with the development of

cardiac hypertrophy [6-11]. The activity of CaMKII is controlled by the phosphorylation at Thr 286/287. Compared to the normal condition, the expression and activity of CaMKII are increased in cardiac hypertrophy and HF, accompanied with the over-expression of ANP, BNP, and MYH7, which are all well-characterized cardiac hypertrophy markers. Once hyperphosphorylation of CaMKII appears, histone deacetylase 4 (HDAC4), the downstream of CaMKII, can also be phosphorylated. HDAC4 is a member of class II histone deacetylases (HDACs), which could promote chromatin condensation and favor transcriptional repression. After phosphorylation of serines in its N terminal of HDAC4 by CaMKII, HDAC4 ceased its inhibition of myocyte enhancer factor-2 (MEF2) and was bound with the chaperone protein 14-3-3, which cooperates with Chromosomal Maintenance 1 (CRM1)/exportin1 to redistribute HDAC4 from nuclear to the cytoplasm [12, 13]. MEF2 has emerged as an important and critical target transcription factor of HDAC4 and has been reported to enhance hypertrophic gene transcription [14-19]. The signal response of MEF2 was influenced by the nucleus-to-cytoplasm shuttling of HDAC4. HDAC4 located in the nucleus could bind with MEF2, which prevents the activation of fetal gene program by maintaining the relevant DNA in a condensed chromatin conformation [20]. Meanwhile, HDAC4 located in the cytoplasm could leave MEF2 to bind with histone acetylases HATs, which can then lead to open chromatin conformation and activate the fetal gene program. In general, once CaMKII is activated, it phosphorylates and drives the nucleus-to-cytoplasm shuttling of HDAC4, which triggers the activation of MEF2. These reactions work together in the development of HF [21].

Yimucao *(Leonurus japonicas Houtt)* is a traditional Chinese medicine, which was originally recorded in "Shennong Bencao Jing". It is a kind of fresh or dried ground parts in the Labiaceae family. It is grown in the mountains, grass of the river bank and the wet place of the stream, which are widely distributed throughout the China. Yimucao enters the liver, pericardium and bladder meridian and has the function of activating blood, regulating menstruation, diuresis detumescence, and clearing heat and detoxication (The Chinese Pharmacopoeia, 2020 version, page 303). Since ancient times, it has been used for the treatment of menstrual disorders, dysmenorrhea and other gynecological diseases in China. Modern pharmacological research displays that Yimucao has certain therapeutic effects on the cardiovascular system in addition to treating gynecological diseases [22, 23]. Stachydrine hydrochloride (Sta) is an activated alkaloid isolated from Yimucao. Our laboratory has also shown that Sta attenuates angiotensin II (AngII)-induced cardiomyocyte hypertrophy, norepinephrine-induced cardiomyocyte hypertrophy and pressure overload-induced cardiac hypertrophy [24-26]. It has also been revealed that the obvious anti-hypertrophic effects of Sta might be attributed to the regulation of calcium handling and the activity of CaMKII [27]. However, the detailed anti-hypertrophic mechanism of Sta is not fully elucidated. Here, we aimed to provide detailed research regarding the anti-hypertrophic effects of Sta on transcriptional factors.

Materials and methods

Chemicals and reagents

Stachydrine hydrochloride (Sta, Cas:4136-37-2, >98%) was purchased from the National Institutes for Food and Drug Control (Beijing, China). Trichostatin A (TSA, Cas:58880-19-6, >97%) was purchased from Selleck (Shanghai, China).

Experimental animals

All experimental protocols were approved by the Animal Care and Use Committee of Shanghai University of Traditional Chinese Medicine (Shanghai, China, PZSHUTCM2007-03008). Adult male C57BL/6J mice (7 weeks) were purchased from Beijing Vital River Laboratory Animal Technology Co, Ltd. (Beijing, China). The mice were housed in cages with controlled temperature and humidity, 12 h light-dark periods, and free access to water and diet. Prior to the experiments, all mice were given a period of about 7 days for acclimatization.

Treatments and establishment of TAC

The transverse aorta constriction (TAC) surgery was used to generate pressure overload induced cardiac hypertrophy. Briefly, mice were placed in a chamber with 5% isoflurane to

induce anesthesia. Then the mice were placed supine on a warming platform (37°C) and were maintained under anesthesia by 1% isoflurane. The aorta between the innominate artery and the left carotid artery was constricted with a ligature tied around a bent 27-gauge needle, and then the needle was quickly removed, creating partial aortic constriction. The sham group underwent all operation procedures except the ligation. After three days of TAC, the sham surgery group received normal saline and the TAC surgery group was randomized to normal saline, Sta (12 mg/kg), or Sta (6 mg/kg), once a day by oral administration for a period of 4 weeks.

Cell culture and treatment

H9c2 culture and treatment: The cell line was purchased from the Shanghai Institute of Cell Biology (Shanghai, China). Cells were cultured in Dulbecco's Modified Eagle's Medium supplemented with 10% FBS at 37°C in a 5% CO_2 incubator. Then the cells were exposed to the following conditions for 48 h: control group (Con), PE (50 μM) group, PE+Sta (5×10^{-5} M), PE+Sta (10^{-5} M), PE+TSA (10^{-7} M).

Adult mouse cardiac myocytes (AMCMs) isolation, culture and treatment: Adult C57BL/6J mice were anesthetized and the heart was removed and perfused on the Langendorff apparatus with Ca^{2+}-free Tyrode's solution at 37°C for 5 min. After that, the heart was digested with Tyrode's solution containing collagenase (300 U/ml, Worthington, Lakewood, NJ, USA) and 50 μM Ca^{2+} for about 10 min. The concentration of Ca^{2+} was gradually increased from 12.5 μM to 900 μM over a period of 30 min, and the cardiomyocytes were harvested. The rod-shaped and quiescent AMCMs were cultured in M199 medium and were treated as follows for 12 h: control group (Con), PE (50 μM) group, PE+Sta (5×10^{-5} M), PE+Sta (10^{-5} M), PE+TSA (10^{-7} M).

Echocardiography analysis

The mice were anesthetized with 1% isoflurane. LV function was evaluated by echocardiography using a small animal imaging system (Vevo2100, Visual Sonics Inc, Toronto, Canada), with the animal situated in the supine position on a warming platform (37°C). The left ventricular (LV) dimensions were assessed in parasternal short-axis at the level of the papillary muscles. The ejection fraction (EF), fractional shortening (FS), LV end-systolic diameter (LVESd), LV end-diastolic diameter (LVEDd), interventricular septal thickness at end-diastole (IVSd), interventricular septal thickness at end-systole (IVSs), LV posterior wall thickness at end-diastole (LVPWd), and LV posterior wall thickness at end-systole (LVPWs) were measured.

Tissue collection

At the end of the study, after the echocardiography analysis and while the mice were still anesthetized, the heart was quickly removed and washed with cold phosphate buffered saline (PBS). After being photographed and weighed, the heart was collected. Meanwhile, the lungs and tibia length (TL) were also weighed and measured. Heart weight (HW) and lung weight (LW) were normalized to TL.

Histologic analysis

Tissue samples were rinsed in PBS, fixed in 4% paraformaldehyde overnight at 4°C, followed by paraffin embedding, and then serially sectioned at a thickness of 5 μm for histological analysis. To assess the cross sectional area of cardiomyocytes (CSA), sections were stained with hematoxylin and eosin (HE) and wheat germ agglutinin (WGA, Life Technologies, New York, NY, USA). Microscopic images were captured with a digital microscope (Zeiss, Jena, Germany).

In vitro H9c2 area measurement was performed according to established procedures. The cytoskeletal actin stained with FITC-phalloidin (Yeasen, Shanghai, China) was examined by a confocal microscope (Zeiss, Jena, Germany) and relative cell area was analyzed by Zen system (Zeiss, Jena, Germany).

Immunofluorescence staining

The AMCMs were fixed with 4% paraformaldehyde for 10 min, washed twice with PBS and incubated with primary antibodies (p-CaMKII (T287): 1:200, Abcam, Cambridge, CB, UK; anti-HDAC4: 1:200, Abcam, Cambridge, CB, UK) overnight at 4°C. The next day, the cells were incubated with the Alexa Fluor (green;

Table 1. Primer sequences for RT-PCR analysis

primer	Forward primer 5'-3'	Reverse primer 5'-3'
ANP (mouse)	CGTCTTGGCCTTTTGGCTTC	GGTGGTCTAGCAGGTTCTTGAAA
BNP (mouse)	GGAGAACACGGCATCATTGC	CTCCAGCAGCTTCTGCATCT
MYH7 (mouse)	CTACCCTCAGGTAGGAGTGGGA	TCTCGGAGCCACCTTGGAAC
MEF2C (mouse)	ACGATTCAGTAGGTCACAGCC	GGAGGTGGAACAGCACACAA
GAPDH (mouse)	ACCCTTAAGAGGGATGCTGC	CCCAATACGGCCAAATCCGT
ANP (rat)	GCCGAGACAGCAAACATCAG	AGGTGGTCTAGCAGGTTCTTGAAA
BNP (rat)	AGCTCTCAAAGGACCAAGGC	AAAACAACCTCAGCCCGTCA
MYH7 (rat)	GCCCCATATATACAGCCCCTG	CCATGACTGAGCCTTGGATT
MEF2C (rat)	CTCGGACATTGTGGAGGCAT	GGAGGTGGAACAGCAGGAAT
GAPDH (rat)	CTCTCTGCTCCTCCCTGTTC	CGATACGGCCAAATCCGTTC

CST, Danvers, MA, USA) for 1 h at room temperature in dark, and then stained with DAPI (blue; Sigma, St. Louis, MO, USA). Finally, images were obtained at 488 nm excitation by a Carl Zeiss LSM800 confocal microscope (Zeiss, Jena, Germany).

Western blotting analysis

The proteins were extracted by cold lysis buffer from LV and cells respectively, or LV was lysed using nucleus and cytoplasmic extraction reagents (Pierce Biotechnology, Rockford, IL, USA). Proteins were determined with a BCA Protein Assay Kit (Beyotime, Shanghai, China). The protein lysates were separated via 10% SDS-PAGE and then transferred to PVDF (0.45 μm, EMD Millipore, Billerica, MA, USA). After being blocked with 5% nonfat milk, the membranes were incubated with the following antibodies overnight at 4°C: anti-HDAC4 (1:1000, Abcam, Cambridge, CB, UK), anti-p-HDAC4 (1:1000, Abcam, Cambridge, CB, UK), anti-CaMKII (1:1000, Abcam, Cambridge, CB, UK), anti-p-CaMKII (T287) (1:1000, Abcam, Cambridge, CB, UK), anti-p-CaMKII (T286) (1:1000, Abcam, Cambridge, CB, UK), anti-ox-CaMKII (1:500, Abcam, Cambridge, CB, UK), anti-MEF2C (1:1000, Abcam, Cambridge, CB, UK), anti-GAPDH (1:3000, Proteintech, Rosemont, IL, USA), or anti-β-tubulin (1:1000, CST, Danvers, MA, USA). The next day, the membranes were incubated with appropriate secondary antibodies. At last, signals were detected using a chemiluminescence reagent (EMD Millipore, Billerica, MA, USA). The protein band densities were quantified by Image J software and expressed as ratios to GAPDH or β-tubulin.

Real-time PCR

Total RNA was isolated from frozen mouse LV tissues or H9c2 using Trizol reagent (Beyotime, Shanghai, China), and reverse transcribed to cDNA using the PrimeScript RT reagent kit with gDNA Eraser (Takara, Japan). Next, real-time PCR was performed using SYBR green (Takara, Japan). Amplification was monitored using the RT-PCR system (QuantStudio 3, ABI, USA). The results were analyzed with the $2^{-\Delta\Delta Ct}$ method and normalized against GAPDH gene expression. The primer sequences were used as follows (**Table 1**).

MEF2-luciferase assays

MEF2 transcriptional activity was estimated by dual-luciferase reporter assay. H9c2 cells were seeded at a density of 5000 cells/well in 96 well plates 1 day prior to transfection. Cells were co-transfected with the pGMMEF2-Luc reporter plasmid (Yeasen, Shanghai, China) and control plasmid pGMLR-TK expressing Renilla reniformis luciferase reporter gene (Yeasen, Shanghai, China). Transfection was performed using Lipofectamine 2000 (Invitrogen, Carlsbad, CA, USA) following the protocol. After 8 h incubation, cells were treated with or without PE and Sta for an additional 24 h. Cells were then lysed and a luciferase assay was performed with the dual luciferase kit (Yeasen, Shanghai, China) according to the manufacturer's instructions. Luciferase measurements were normalized to the corresponding renilla activities for transfection efficiency.

Statistical analysis

The data were presented as means ± SEM. Statistical comparisons were performed by

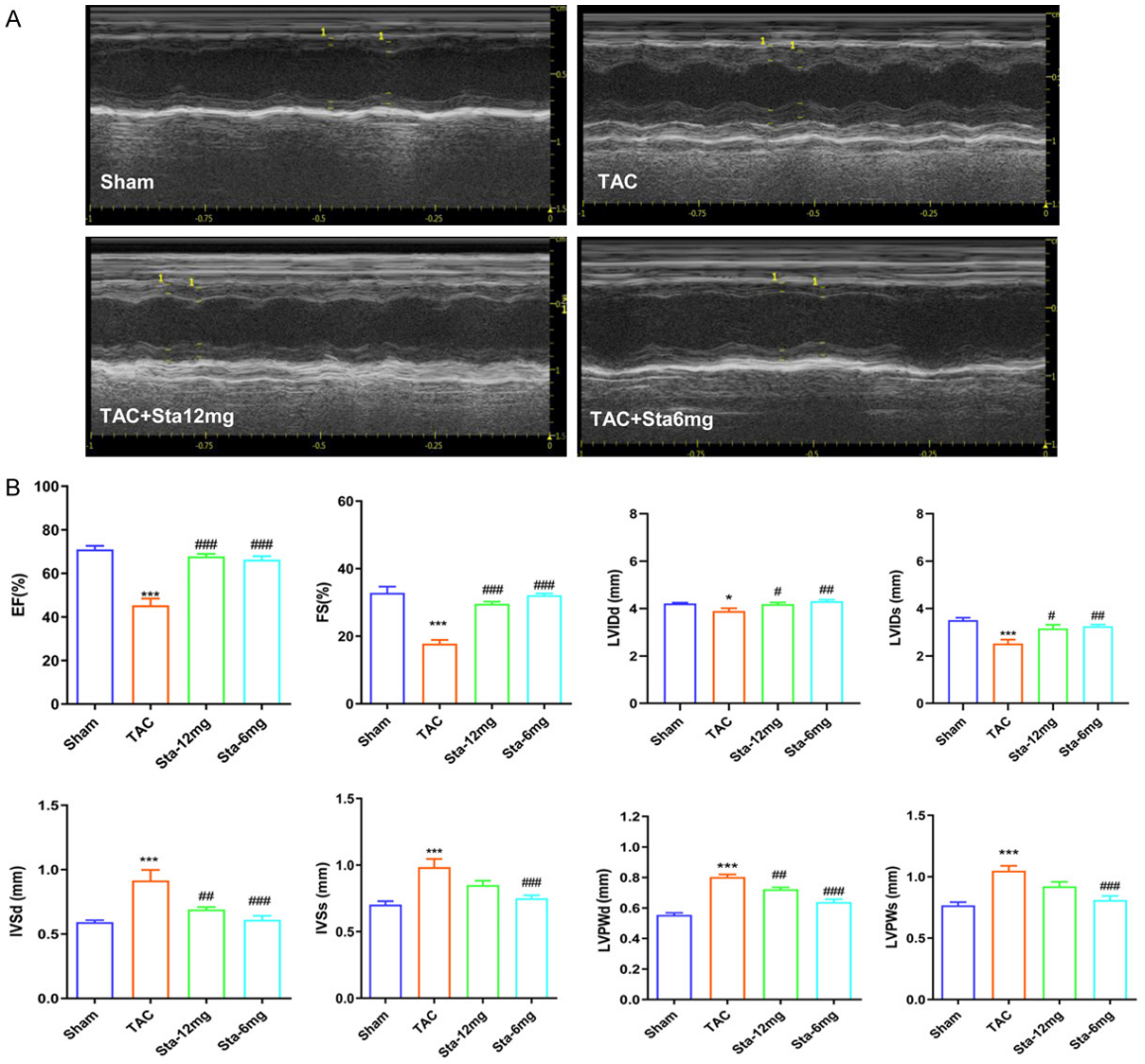

Figure 1. Sta improves pressure overload-induced LV remodeling and cardiac dysfunction. A: The echocardiography (ECG) was examined at 4W after TAC. B: Statistical quantification of ECG parameters. *P<0.05 vs. Sham, ***P<0.001 vs. Sham; #P<0.05 vs. TAC, ##P<0.01 vs. TAC, ###P<0.001 vs. TAC. EF: ejection fraction, FS: fractional shortening, LVESd: LV end-systolic diameter, LVEDd: LV end-diastolic diameter, IVSd: interventricular septal thickness at end-diastole, IVSs: interventricular septal thickness at end-systole, LVPWd: LV posterior wall thickness at end-diastole, LVPWs: LV posterior wall thickness at end-systole, TAC: transverse aorta constriction, Sta: Stachydrine hydrochloride.

one-way analysis of variance (ANOVA) followed by Tukey's post hoc analysis using GraphPad Prism 8 software, and differences were considered significant at P<0.05.

Results

Sta alleviated TAC-induced cardiac dysfunction in mice

The mice were treated with TAC for 4 weeks in the presence or absence of Sta. Echocardiography tests of cardiac performance show that the mice exhibited significantly increased IVSd, IVSs, LVPWd and LVPWs, as well as decreased EF% and FS% after TAC only, which indicates cardiac hypertrophy. However, Sta treatment markedly attenuated the cardiac dilation and LV dysfunction (**Figure 1**). No significant difference in cardiac function was observed between the groups of 6 mg/kg and 12 mg/kg Sta. These data indicate that Sta blocks the pathological cardiac dysfunction induced by chronic pressure overload.

Sta represses cardiac hypertrophy in vivo and in vitro

Compared with the sham group, the mice subjected to TAC only developed cardiac hypertrophy as indicated by increased HW/BW and HW/TL ratios. Whereas, the mice with the treatment of Sta had less increase in heart size. The increased HW/BW and HW/TL ratios induced by TAC were also abrogated by Sta and did not differ from the sham group (**Figure 2Aa**, **2Ab**, **2C**). Similar results were obtained for the cross-sectional area of cardiomyocytes that were measured by histological analysis using HE and WGA (**Figure 2Ac**, **2Ad**, **2D**). In vitro, H9c2 cells were induced by PE after being treated with or without Sta and TSA. As shown in **Figure 2B** and **2E**, treatment of Sta or TSA decreased the surface area of PE-induced cells. The fetal genes, such as ANP, BNP, and MYH7 were all elevated in mRNA in the TAC-induced mouse heart and PE-induced H9c2 cells, and administration of Sta significantly reduced the mRNA of these genes in vivo and in vitro (**Figure 2F**, **2G**).

Sta abolished CaMKII activity in vivo and in vitro

Although phosphorylation and oxidation of CaMKII are the parameters for monitoring CaMKII activity, phosphorylation at Thr287 is a well-established parameter in the heart. First, we test the expression of p-CaMKIIδ (T287) by immunofluorescence in vitro. As shown in **Figure 3A**, the expression of p-CaMKIIδ (T287) was significantly increased in the PE group. The treatment with Sta significantly inhibited the high expression of p-CaMKIIδ (T287) induced by PE, while there was no difference in the expression of p-CaMKIIδ (T287) between TAS treatment and PE only. Then, we tested the protein expression of phosphorylated CaMKIIδ by western blotting (**Figure 3B**, **3D**) in H9c2 cells. Accompanied with immunofluorescence, similar results were obtained for the western blotting. We observed that the protein expression of p-CaMKIIδ (T287) significantly increased in PE. In addition, we found that the expression of ox-CaMKIIδ also increased in PE. Though Sta could inhibit increased expression of p-CaMKIIδ (T287) and ox-CaMKIIδ induced by PE, TSA has no effect on the phosphorylation of CaMKIIδ. However, we also found that the expressions of p-CaMKIIδ (T287) and ox-CaMKIIδ increased in the TAC only group, while these changes were attenuated by the treatment of Sta (**Figure 3C**, **3E**).

Sta inhibits the phosphorylation and nuclear translocation of HDAC4 in vivo and in vitro

To determine whether PE induced the HDAC4 nuclear export, we tested the subcellular distribution of HDAC4 in AMCMs and H9c2 cells (**Figure 4A**). We found that HDAC4 was located in both the cytoplasm and nucleus, but the major expression resided within the nucleus in the control group. After PE stimulation, the immunofluorescence that was localized in the nucleus was weakened, and the fluorescence intensity in the cytoplasm was increased. The treatment with Sta or TSA could prevent the change of fluorescence intensity in the cytoplasm and nuclei induced by PE. Then, we de tected the protein expression of HDAC4 in the cytoplasm and nucleus, respectively. We extracted nucleus proteins and cytoplasmic proteins from the heart tissue. The results showed that, in the mice subjected to TAC only, the expression of HDAC4 distinctly decreased in nucleus, accompanied by an increase in the cytoplasm. Similar effects of Sta in vitro were observed in vivo (**Figure 4B-E**). The phosphorylation of serines in its N terminal of HDAC4 results in the binding of the chaperone protein 14-3-3, which cooperates with CRM1/exportin1 to redistribute HDAC4 to the cytoplasm. As shown in **Figure 4F** and **4G**, the expression of p-HDAC4 (S632) was significantly increased in the mice subjected to TAC only, and the treatment with Sta could inhibit a high expression of p-HDAC4 (S632). In vitro, we also found that Sta and TSA obviously inhibited the increase of p-HDAC4 (S632) induced by PE (**Figure 4H**, **4I**).

Sta inhibited the activation of MEF2C in vivo and in vitro

To investigate the effect of Sta on MEF2 activity, H9c2 cells were transfected with a MEF2 luciferase reporter plasmid. As shown in **Figure 5A**, the activity of MEF2 was enhanced in the PE only group. Here, treatment with Sta or TSA abolished the increase of MEF2 activity that was measured in response to the PE stimulant. Next, we observed the mRNA and protein levels of MEF2C in vitro. As shown in **Figure 5B**, the mRNA level of MEF2C in H9c2 cells treated with PE only was significantly increased com-

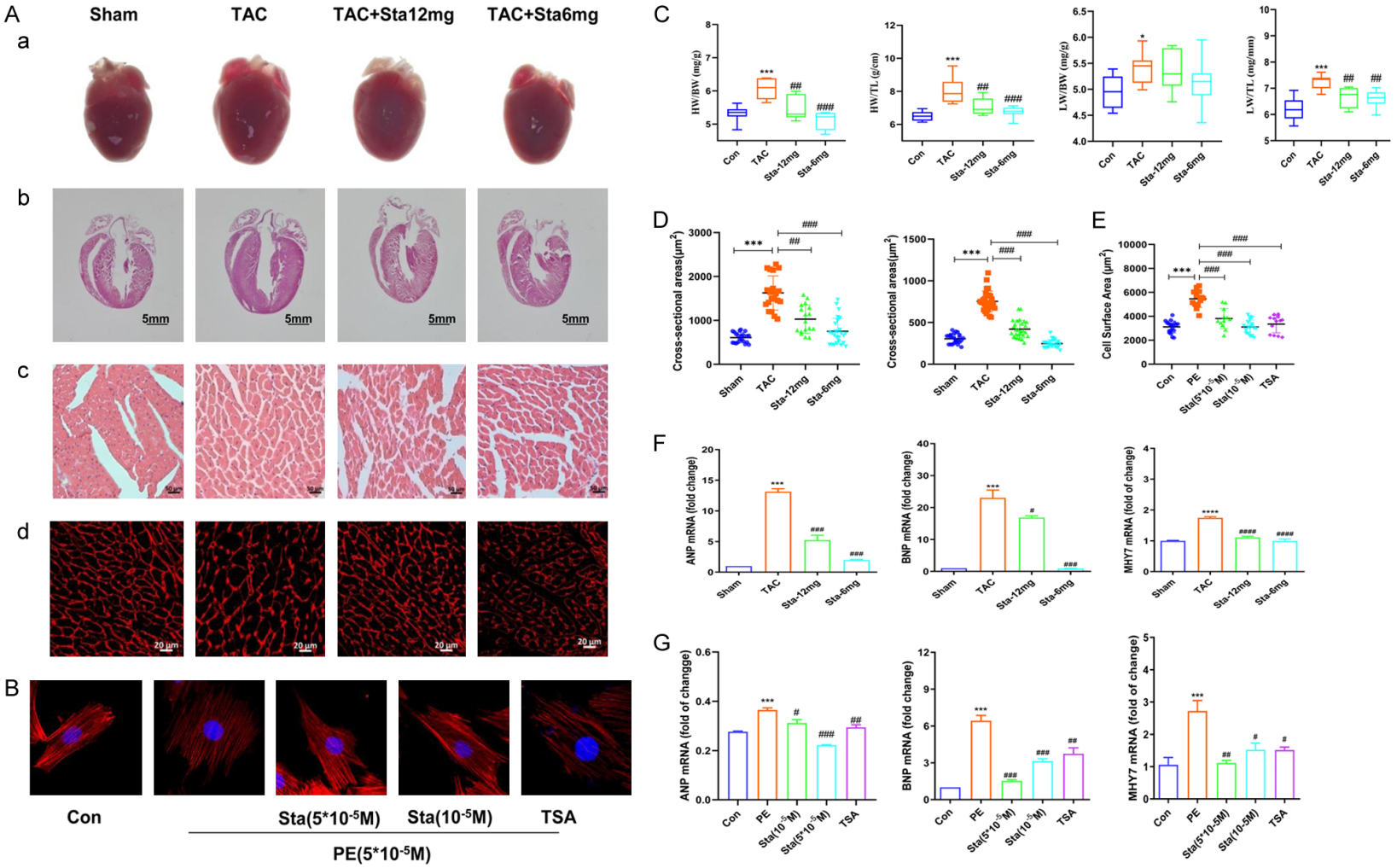

Figure 2. Sta alleviates myocardial hypertrophy in vivo and in vitro. A: (a) heart photos, (b, c) Representative HE staining in global and in details, (d) Representative WGA staining. B: Representative immunofluorescence images showing α-actinin staining in NRCMs. C: Heart weight and lung weight normalized to body weight (HW/BW, LW/BW) or tibia length (HW/TL, LW/TL). D: Statistical quantification of CSA stained with HE and WGA respectively. E: Statistical quantification of cell surface area stained with α-actinin. F: mRNA expression of ANP, BNP, and MYH7 in LV tissue. G: mRNA expression of ANP, BNP, and MYH7 in H9c2 cells. *P<0.05 vs. Sham or Con, ***P<0.001 vs. Sham or Con; #P<0.05 vs. TAC or PE, ##P<0.01 vs. TAC or PE, ###P<0.001 vs. TAC or PE. HW: heart weight; LW: lung weight; TL: tibia length; CSA: cross sectional area of cardiomyocytes; WGA: heat germ agglutinin; TAC: transverse aorta constriction; PE: Phenylephrine; Sta: Stachydrine hydrochloride.

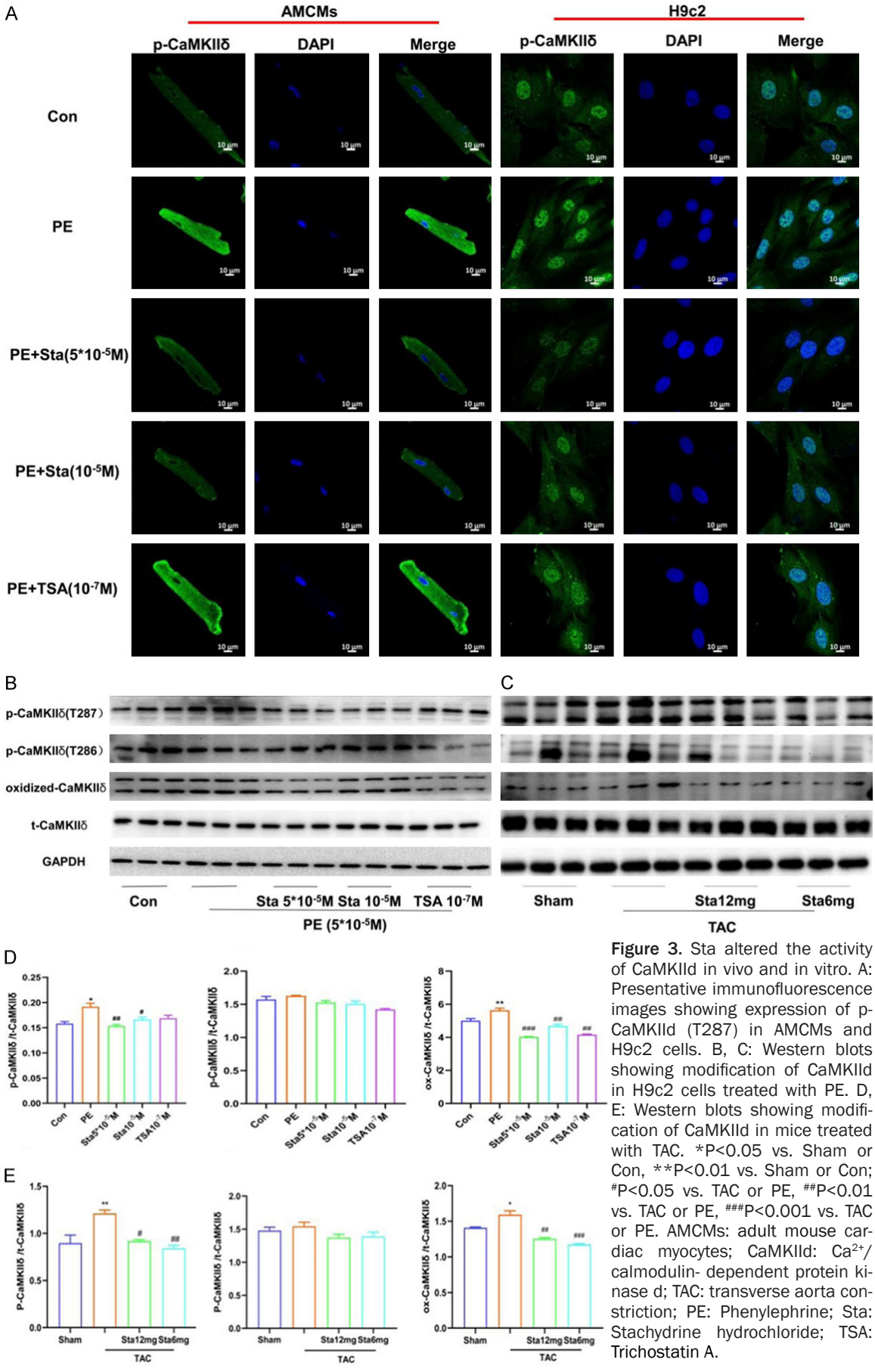

Figure 3. Sta altered the activity of CaMKIId in vivo and in vitro. A: Presentative immunofluorescence images showing expression of p-CaMKIId (T287) in AMCMs and H9c2 cells. B, C: Western blots showing modification of CaMKIId in H9c2 cells treated with PE. D, E: Western blots showing modification of CaMKIId in mice treated with TAC. *P<0.05 vs. Sham or Con, **P<0.01 vs. Sham or Con; #P<0.05 vs. TAC or PE, ##P<0.01 vs. TAC or PE, ###P<0.001 vs. TAC or PE. AMCMs: adult mouse cardiac myocytes; CaMKIId: Ca^{2+}/calmodulin- dependent protein kinase d; TAC: transverse aorta constriction; PE: Phenylephrine; Sta: Stachydrine hydrochloride; TSA: Trichostatin A.

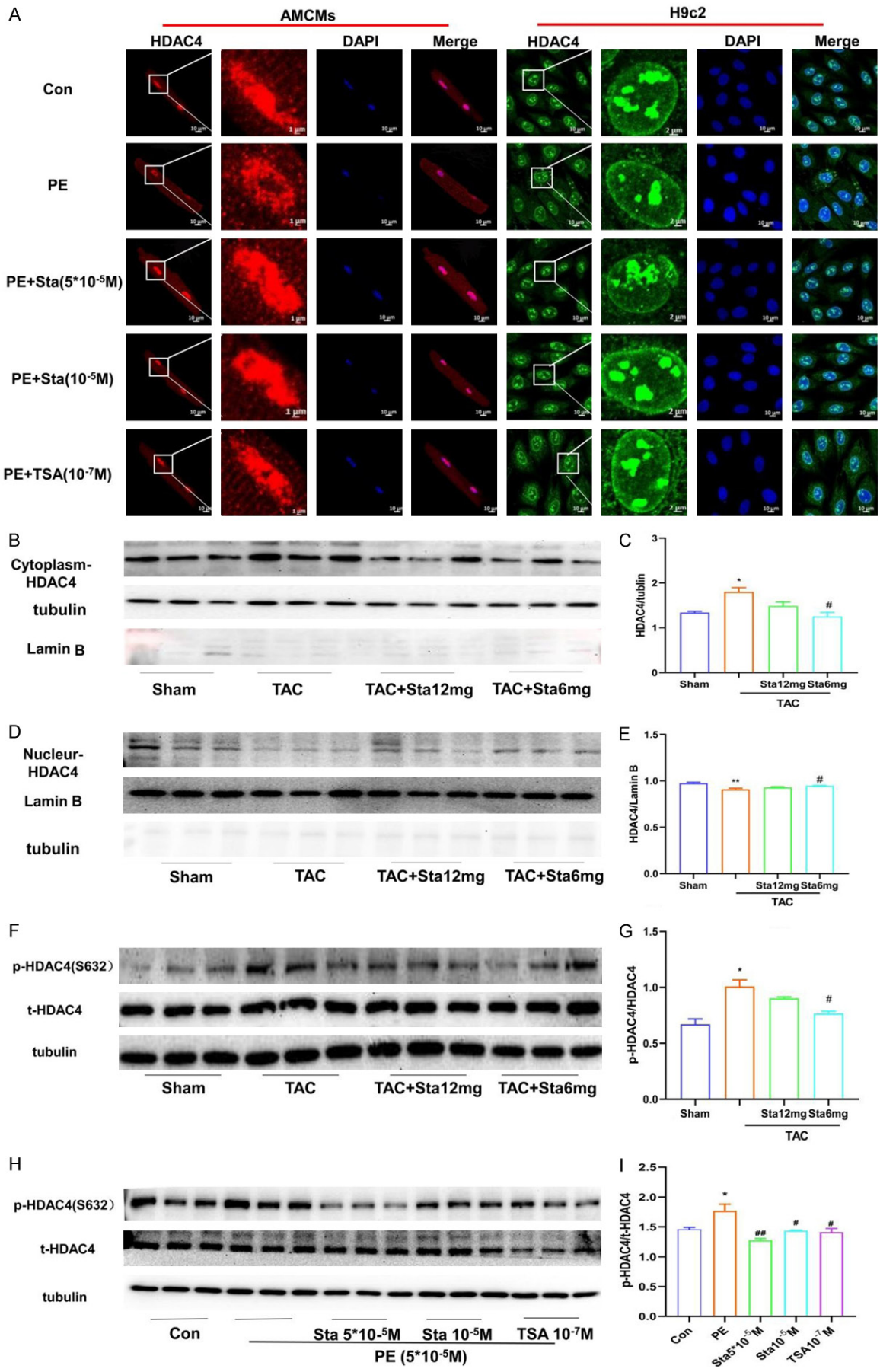
A
AMCMs
H9c2
HDAC4
DAPI
Merge
Con
PE
PE+Sta(5*10-5M)
PE+Sta(10-5M)
PE+TSA(10-7M)
B
Cytoplasm-HDAC4
tubulin
Lamin B
Sham
TAC
TAC+Sta12mg
TAC+Sta6mg
C
HDAC4/tublin
Sta12mg Sta6mg
TAC
D
Nucleur-HDAC4
E
HDAC4/Lamin B
F
p-HDAC4(S632)
t-HDAC4
G
p-HDAC4/HDAC4
H
Con
Sta 5*10-5M
Sta 10-5M
TSA 10-7M
PE (5*10-5M)
I
p-HDAC4/t-HDAC4

Figure 4. Sta altered the phosphorylation and nuclear export of HDAC4 in vivo and in vitro. A: Presentative immunofluorescence images showing distribution of HDAC4 in AMCMs and H9c2 cells. B-E: Western blots showing expression of HDAC4 in the cytoplasm and nucleus in mice treated with TAC. F, G: Western blots showing modification of HDAC4 in mice treated with TAC. H, I: Western blots showing modification of HDAC4 in H9c2 cells treated with PE. *P<0.05 vs. Sham or Con; #P<0.05 vs. TAC or PE, ##P<0.01 vs. TAC or PE. AMCMs: adult mouse cardiac myocytes; HDAC4: histone deacetylase 4; TAC: transverse aorta constriction; PE: Phenylephrine; Sta: Stachydrine hydrochloride.

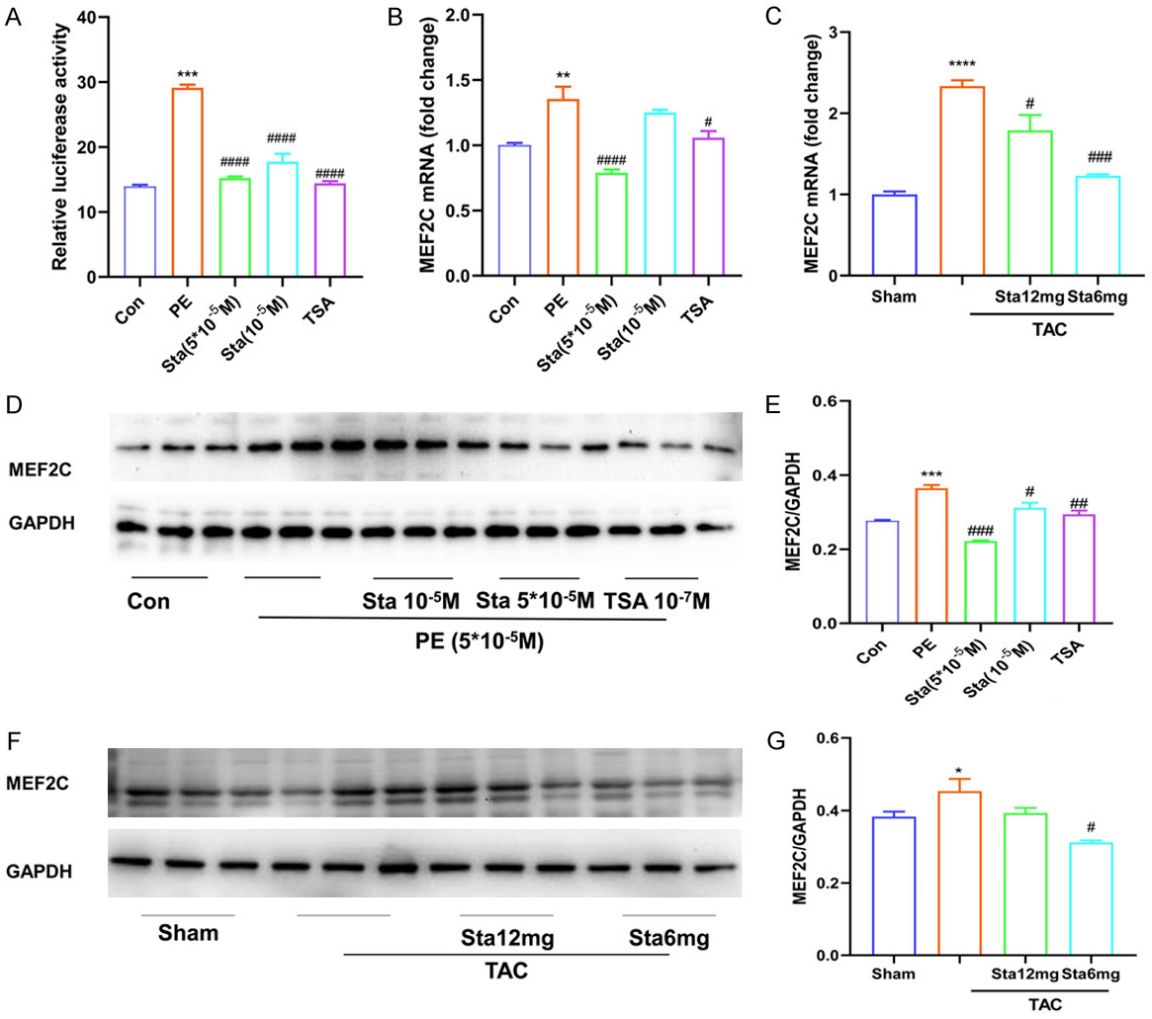

Figure 5. Sta inhibited MEF2 activity in vivo and in vitro. A: MEF2 activity is expressed as MEF2-Luc to Renilla luciferase ratio in H9c2 cells treated with PE. B: mRNA expression of MEF2C in H9c2 cells treated with PE. C: mRNA expression of MEF2C in mice treated with TAC. D, E: Western blots showing expression of MEF2C in H9c2 cells treated with PE. F, G: Western blots showing expression of MEF2C in mice treated with TAC. *P<0.05 vs. Sham or Con, ***P<0.001 vs. Sham or Con; #P<0.05 vs. TAC or PE, ##P<0.01 vs. TAC or PE, ###P<0.001 vs. TAC or PE. MEF2: myocyte enhancer factor-2; TAC: transverse aorta constriction; PE: Phenylephrine; Sta: Stachydrine hydrochloride.

pared to the control group, and a similar change was found in the protein level of MEF2C (**Figure 5D**, **5E**). In vivo, compared to the sham group, the mRNA and proteins of MEF2C were all increased in the TAC mice (**Figure 5C**, **5F**, **5G**). Both the mRNA and protein levels of MEF2C were significantly reduced with the treatment of Sta in vivo and vitro (**Figure 5**).

Discussion

In cardiac muscle, abnormal Ca^{2+} handling could contribute to heart dysfunction [28]. CaMKII, as one of the cellular decoder of Ca^{2+} signals, plays a vital role in cardiac diseases such as hypertrophic growth [4, 5]. In our previous work, we revealed that with calcium mis-

handling and hyper-phosphorylation of CaMKII in TAC-induced cardiac hypertrophy, Sta could reverse these changes [27], while the signal of downstream remained unclear. In this study, we aimed to elaborate on the cardiac protective effect of Sta via transcriptional regulation.

CaMKII has been implicated in the transcriptional regulation associated with the development of cardiac hypertrophy [6-11]. CaMKII could phosphorylate downstream proteins such as histone deacetylases (HDACs). HDACs remove the acetyl group from histone lysine residues, inducing chromatin condensation and transcriptional repression [29]. In the past few years, some studies have reported that chronic HDAC inhibition could attenuate cardiac hypertrophy [29-31]. HDACs consist of 18 enzymes, and could be further classified into four classes: I, II, III, and IV. The activities of these enzymes have some important effects on different physiological and pathological phenomena, including cell growth, differentiation, intracellular signal transduction and more [31-35]. HDAC4 is a member of class IIa HDACs, which are highly expressed in the heart, and it plays a key role in the progression of the pathological hypertrophy [36]. HDAC4 possesses a long N-terminal contains some binding sites for MEF2, 14-3-3, calcium responsive phosphorylation sites, and a nuclear localization signal (NLS); its C-terminal contains a deacetylase domain and a nuclear export signal (NES). The phosphorylation of serine phosphorylation sites (246, 467, and 632) in the N-terminal regions of HDAC4 could result in the binding of protein 14-3-3, which cooperates with CRM1/exportin1 to redistribute HDAC4 from nucleus to the cytoplasm [12, 37]. In the nucleus, HDAC4 joins with MEF2, which plays a vital role in preventing reactivation of the fetal gene program by maintaining the DNA in a condensed chromatin conformation [36]. In the cytoplasm, HDAC4 leads to a dissociation of the repressor complexes and activates gene transcription by derepression of transcription factors [19, 29]. Thus, the localization of HDAC4 strictly determines its function in myocytes. The phosphorylated HDAC4 is not available to import in the nucleus unless dephosphorylated by phosphatases like PP2A. After that, dephosphorylated HDAC4 escapes from the control of the 14-3-3 protein and shuttles into the nucleus, localizing in the transcription factor promoter region and inhibiting its expression [38]. In this study, we described the protective effects of Sta against cardiac hypertrophy, accompanied by the inhibition of cardiomyocyte enlargement and significant increase in hypertrophic gene expression (**Figures 1**, **2**). We also found that the hyper-phosphorylation of CaMKII was decreased in response to the treatment with Sta in vivo and in vitro (**Figure 3**). A number of studies have delineated the major importance of CaMKII in the development of cardiac hypertrophy and have shown that CaMKII signals specifically to HDAC4 but not other HDACs [38]. Once hyper-phosphorylation of CaMKII appeared, as the downstream of CaMKII, HDAC4 could be phosphorylated. CaMKII signals selectively to HDAC4 by docking to a domain that is uniquely present in HDAC4-serine 632 [39]. In our study, we found that HDAC4 was located in both the cytoplasm and nucleus, but the major expression resided within the nucleus under normal conditions. After the stimulation of PE on AMCMs and H9c2, the translocation of HDAC4 was very apparent (**Figure 4**). Consistent with these findings, we observed that the protein expression of HDAC4 in the cytoplasm was much higher in the mice subjected to TAC only. These results confirmed HDAC4 nuclear translocation during cardiac hypertrophy induced by pressure overload. Meanwhile, we found that the levels of p-HDAC4 (S632) were higher in vivo and in vitro after the stimulation of TAC or PE (**Figure 4**). In summary, phosphorylation of HDAC4 promoted the nuclear export and prevented the nuclear import of HDAC4, and CaMKII played a significant role in determining the phosphorylation and localization of HDAC4. Additionally, Sta repressed the activation of HDAC4, and inhibited its nucleus-to-cytoplasm shuttling.

The transcriptional activity of MEF2 is tightly governed by HDAC4 [15], and its downstream target genes are involved in cardiac remodeling [14]. MEF2 is a member of the MADS-box-family of transcription factors that regulate cardiac myocyte growth and differentiation [40]. MEF2C is one specific MEF2 isoform, which functions as a mediator of cardiac and skeletal muscle differentiation and growth [34, 41]. MEF2C has emerged as an important and critical target transcription factor of HDAC4 and it has been suggested that it acts as a common end point for hypertrophic signaling pathway in the myocardium [14-19]. HDAC4 located in the cytoplasm leaves MEF2C to bind with HATs, which could lead to open chromatin conformation and activate the fetal gene program. In

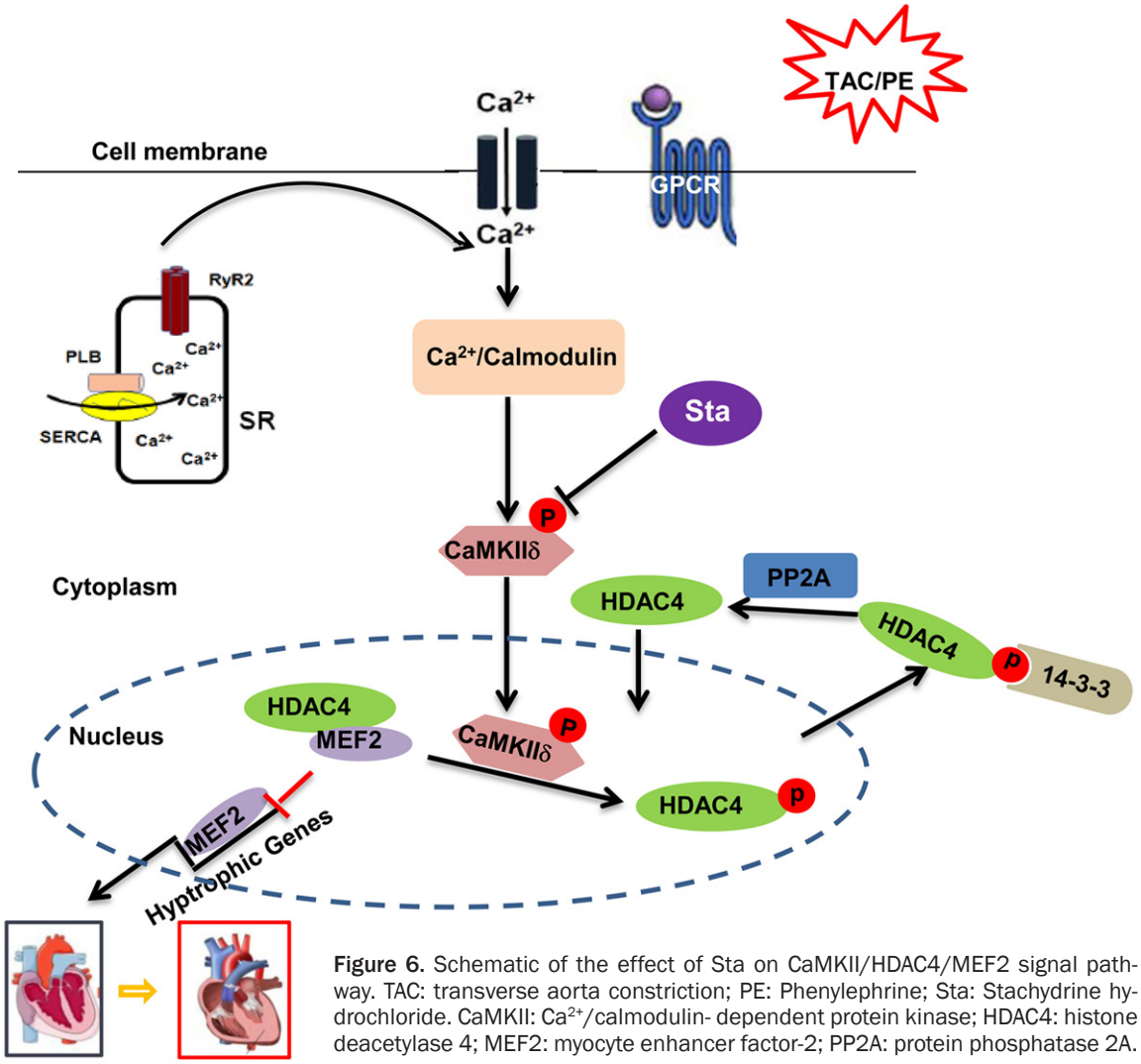

Figure 6. Schematic of the effect of Sta on CaMKII/HDAC4/MEF2 signal pathway. TAC: transverse aorta constriction; PE: Phenylephrine; Sta: Stachydrine hydrochloride. CaMKII: Ca^{2+}/calmodulin- dependent protein kinase; HDAC4: histone deacetylase 4; MEF2: myocyte enhancer factor-2; PP2A: protein phosphatase 2A.

our results, the MEF2 luciferase reporter has shown that the activity of MEF2 was obviously increased in H9c2 cells treated with PE only, while the treatment with Sta or TSA (the non-selective HDAC inhibitor trichostatin A) inhibited the activity of MEF2. The mRNA and protein of MEF2C were also decreased by treatment with Sta or TSA (**Figure 5**). Under normal conditions, MEF2C is constitutively associated with HDAC4, which maintains MEF2C in a transcriptionally inactive state [19]. The results in our study were consistent with literature reports.

Conclusion

Cardiac-specific activation of the CaMKII/HDAC4/MEF2C pathway is sufficient to induce myocardial hypertrophy (**Figure 6**). Additionally, Sta has cardioprotective effects. The results of the present study revealed that Sta inhibited nuclear export or promoted nuclear import of HDAC4 through regulation of p-CaMKII, and further improved the repression of MEF2C. In summary, Sta ameliorates cardiac hypertrophy induced by pressure overload through the CaMKII/HDAC4/MEF2C signal pathway, which reveals a novel mechanism for the cardioprotective effect of Sta on transcriptional reprogramming.

Acknowledgements

This study was funded by the National Natural Science Foundation of China (NO: 82004144; 82074054), and the Budget Research Project of Shanghai Education Commission (NO: 2020LK003).

Disclosure of conflict of interest

None.

Address correspondence to: Rong Lu, School of Basic Medical Science, Shanghai University of Traditional Chinese Medicine, Shanghai 201203, China. Tel: +86-021-5132460; Fax: +86-021-51322460; E-mail: lurong@shutcm.edu.cn; Pei Zhao, Public Laboratory Platform, School of Basic Medical Science, Shanghai University of Traditional Chinese Medicine, Shanghai 201203, China. Tel: +86-021-5132460; Fax: +86-021-51322460; E-mail: zp1737@sina.com

References

[1] Frey N and Olson EN. Cardiac hypertrophy: the good, the bad, and the ugly. Annu Rev Physiol 2003; 65: 45-79.

[2] Shimizu I and Minamino T. Physiological and pathological cardiac hypertrophy. J Mol Cell Cardiol 2016; 97: 245-262.

[3] Benjamin EJ, Virani SS, Callaway CW, Chamberlain AM, Chang AR, Cheng S, Chiuve SE, Cushman M, Delling FN, Deo R, de Ferranti SD, Ferguson JF, Fornage M, Gillespie C, Isasi CR, Jiménez MC, Jordan LC, Judd SE, Lackland D, Lichtman JH, Lisabeth L, Liu S, Longenecker CT, Lutsey PL, Mackey JS, Matchar DB, Matsushita K, Mussolino ME, Nasir K, O'Flaherty M, Palaniappan LP, Pandey A, Pandey DK, Reeves MJ, Ritchey MD, Rodriguez CJ, Roth GA, Rosamond WD, Sampson UKA, Satou GM, Shah SH, Spartano NL, Tirschwell DL, Tsao CW, Voeks JH, Willey JZ, Wilkins JT, Wu JH, Alger HM, Wong SS and Muntner P; American Heart Association Council on Epidemiology and Prevention Statistics Committee and Stroke Statistics Subcommittee. Heart disease and stroke statistics-2018 update: a report from the American Heart Association. Circulation 2018; 137: e67-e492

[4] Zarain-Herzberg A, Fragoso-Medina J and Estrada-Avilés R. Calcium-regulated transcriptional pathways in the normal and pathologic heart. IUBMB Life 2011; 63: 847-855.

[5] Bers DM. Calcium cycling and signaling in cardiac myocytes. Annu Rev Physiol 2008; 70: 23-49.

[6] Grimm M and Brown JH. Beta-adrenergic receptor signaling in the heart: role of CaMKII. J Mol Cell Cardiol 2010; 48: 322-330.

[7] Anderson ME, Brown JH and Bers DM. CaMKII in myocardial hypertrophy and heart failure. J Mol Cell Cardiol 2011; 51: 468-473.

[8] Swaminathan PD, Purohit A, Hund TJ and Anderson ME. Calmodulin-dependent protein kinase II: linking heart failure and arrhythmias. Circ Res 2012; 110: 1661-1677.

[9] Rokita AG and Anderson ME. New therapeutic targets in cardiology: arrhythmias and Ca2+/calmodulin-dependent kinase II (CaMKII). Circulation 2012; 126: 2125-2139.

[10] Fischer TH, Neef S and Maier LS. The Ca-calmodulin dependent kinase II: a promising target for future antiarrhythmic therapies? J Mol Cell Cardiol 2013; 58: 182-187.

[11] Dewenter M, Neef S, Vettel C, Lämmle S, Beushausen C, Zelarayan L, Katz S, von der Lieth A, Meyer-Roxlau S, Weber S, Wieland T, Sossalla S, Backs J, Brown J, Maier L and El-Armouche A. Calcium/calmodulin-dependent protein kinase II Activity Persists During Chronic β-adrenoceptor blockade inexperimental and human heart failure. Circ Heart Fail 2017; 10: e003840.

[12] Little GH, Bai Y, Williams T and Poizat C. Nuclear calcium/calmodulin-dependent protein kinase IIdelta preferentially transmits signals to histone deacetylase 4 in cardiac cells. J Biol Chem 2007; 282: 7219-7231.

[13] Wang AH and Yang XJ. Histone deacetylase 4 possesses intrinsic nuclear import and export signals. Mol Cell Biol 2001; 21: 5992-6005.

[14] Passier R, Zeng H, Frey N, Naya FJ, Nicol RL, McKinsey TA, Overbeek P, Richardson JA, Grant SR and Olson EN. CaM kinase signaling induces cardiac hypertrophy and activates the MEF2 transcription factor in vivo. Clin Invest 2000; 105: 1395-1406.

[15] Backs J and Olson EN. Control of cardiac growth by histone acetylation/deacetylation. Circ Res 2006; 98: 15-24.

[16] Backs J, Backs T, Neef S, Kreusser MM, Lehmann LH, Patrick DM, Grueter CE, Qi X, Richardson JA, Hill JA, Katus HA, Bassel-Duby R, Maier LS and Olson EN. The delta isoform of CaM kinase II is required for pathological cardiac hypertrophy and remodeling after pressure overload. Proc Natl Acad Sci U S A 2009; 106: 2342-2347.

[17] Kolodziejczyk SM, Wang L, Balazsi K, DeRepentigny Y, Kothary R and Megeney LA. MEF2 is upregulated during cardiac hypertrophy and is required for normal post-natal growth of the myocardium. Curr Biol 1999; 9: 1203-1206.

[18] Lu J, McKinsey TA, Nicol RL and Olson EN. Signal-dependent activation of the MEF2 transcription factor by dissociation from histone deacetylases. Proc Natl Acad Sci U S A 2000; 97: 4070-4075.

[19] Wei J, Joshi S, Speransky S, Crowley C, Jayathilaka N, Lei X, Wu Y, Gai D, Jain S, Hoosien M, Gao Y, Chen L and Bishopric NH. Reversal of pathological cardiac hypertrophy via the MEF2-coregulator interface. JCI Insight 2017; 2: e91068.

[20] Miska EA, Karlsson C, Langley E, Nielsen SJ, Pines J and Kouzarides T. HDAC4 deacetylase associates with and represses the MEF2 transcription factor. EMBO J 1999; 18: 5099-5107.

[21] Helmstadter KG, Ljubojevic-Holzer S, Wood BM, Taheri KD, Sedej S, Erickson JR, Bossuyt J and Bers DM. CaMKII and PKA-dependent phosphorylation co-regulate nuclear localization of HDAC4 in adult cardiomyocytes. Basic Res Cardiol 2021; 116: 11.

[22] Liu XH, Pan LL and Zhu YZ. Active chemical compounds of traditional Chinese medicine Herba Leonuri: implications for cardiovascular diseases. Clin Exp Pharmacol Physiol 2012; 39: 274-282.

[23] Mao YS, Shi JQ, Zhu MY, et al. Advances in the study of pharmacological action of Stachydrine. Chinese Journal of Microcirculation 2017; 27: 65-69.

[24] Zhang C, Shan XL, Liao YL, Zhao P, Guo W, Wei HC and Lu R. Effects of stachydrine on norepinephrine-induced neonatal rat cardiac myocytes hypertrophy and intracellular calcium transients. BMC Complement Altern Med 2014; 14: 474.

[25] Guo W, Zhang C, Liao Y, Lv R and Wei H. Effect of Leonurus stachydrine on myocardial cell hypertrophy. Zhong Yao Cai 2012; 35: 940-943.

[26] Cao TT, Chen HH, Dong Z, Xu YW, Zhao P, Guo W, Wei HC, Zhang C and Lu R. Stachydrine protects against pressure overload-induced cardiachypertrophy by suppressing autophagy. Cell Physiol Biochem 2017; 42: 103-114.

[27] Chen HH, Wang SN, Cao TT, Zheng JL, Tian J, Shan XL, Zhao P, Guo W, Xu M, Zhang C and Lu R. Stachydrine hydrochloride alleviates pressure overload-induced heart failure and calcium mishandling on mice. J Ethnopharmacol 2020; 248: 112306.

[28] Coppini R, Ferrantini C, Mugelli A, Poggesi C and Cerbai E. Altered Ca and Na homeostasis in human hypertrophic cardiomyopathy: implications for arrhythmogenesis. Front Physiol 2018; 9: 1391.

[29] Zhang CL, McKinsey TA, Chang S, Antos CL, Hill JA and Olson EN. Class II histone deacetylases act as signal-responsive repressors of cardiac hypertrophy. Cell 2002; 110: 479-488.

[30] Kong Y, Tannous P, Lu G, Berenji K, Rothermel BA, Olson EN and Hill JA. Suppression of class I and II histone deacetylases blunts pressure-overloadcardiac hypertrophy. Circulation 2006; 113: 2579-2588.

[31] Haberland M, Montgomery RL and Olson EN. The many roles of histone deacetylases in development and physiology: implications for disease and therapy. Nat Rev Genet 2009; 10: 32-42.

[32] Kee HJ, Kim GR, Lin MQ, Choi SY, Ryu Y, Jin L, Piao ZH and Jeong MH. Expression of class I and class II a/b histone deacetylase is dysregulated in hypertensive animal models. Korean Circ J 2017; 47: 392-400.

[33] Granger A, Abdullah I, Huebner F, Stout A, Wang T, Huebner T, Epstein JA and Gruber PJ. Histone deacetylase inhibition reduces myocardial ischemia-reperfusion injury in mice. FASEB J 2008; 22: 3549-3560.

[34] Zhang T, Kohlhaas M, Backs J, Mishra S, Phillips W, Dybkova N, Chang S, Ling H, Bers D, Maier L, Olson E and Brown J. CaMKIIdelta isoforms differentially affect calcium handling but similarly regulate HDAC/MEF2 transcriptional responses. J Biol Chem 2007; 282: 35078-35087.

[35] Park SY and Kim JS. A short guide to histone deacetylases including recent progress on class II enzymes. Exp Mol Med 2020; 52: 204-212.

[36] Gupta MP. Factors controlling cardiac myosin-isoform shift during hypertrophy and heart failure. J Mol Cell Cardiol 2007; 43: 388-403.

[37] Wang AH, Grégoire S, Zika E, Xiao L, Li CS, Li H, Wright KL, Ting JP and Yang XJ. Identification of the ankyrin repeat proteins ANKRA and RFXANK as novel partners of class IIa histone deacetylases. J Biol Chem 2005; 280: 29117-29127.

[38] Chen C, Wei X, Wang S, Jiao Q, Zhang Y, Du G, Wang X, Wei F, Zhang J and Wei L. Compression regulates gene expression of chondrocytes through HDAC4 nuclear relocation via PP2A-dependent HDAC4 dephosphorylation. Biochim Biophys Acta 2016; 1863: 1633-1642.

[39] Backs J, Song K, Bezprozvannaya S, Chang S and Olson EN. CaM kinase II selectively signals to histone deacetylase 4 during cardiomyocyte hypertrophy. J Clin Invest 2006; 116: 1853-1864.

[40] Potthoff MJ and Olson EN. MEF2: a central regulator of diverse developmental programs. Development 2007; 134: 4131-4140.

[41] Muñoz JP, Collao A, Chiong M, Maldonado C, Adasme T, Carrasco L, Ocaranza P, Bravo R, Gonzalez L, Díaz-Araya G, Hidalgo C and Lavandero S. The transcription factor MEF2C mediates cardiomyocyte hypertrophy induced by IGF-1 signaling. Biochem Biophys Res Commun 2009; 388: 155-160.